Wet and Dry Accelerated Aging Tests in a Spray Chamber to Understand the Effects of Acid Rain Frequencies on Bronze Corrosion

Liliana Gianni[1,2], Mauro Cavallini[1], Stefano Natali[1] and Annemie Adriaens[2,]*

[1] Department of Chemical Engineering Materials and Environment (DICMA), Sapienza University of Rome, Via Eudossiana 18, 00184 Rome, Italy
[2] Department of Analytical Chemistry, Ghent University, Krijgslaan 281-S12, 9000 Ghent, Belgium
[*]E-mail: annemie.adriaens@ugent.be

We have conducted controlled laboratory experiments using a series of bronze alloys exposed to frequent, repeated wet and dry cycles, to simulate frequent acid rain exposure and study the resultant corrosion processes in bronze artifacts exposed to an outdoor urban environment. To simulate rainwater and condensation, a spray chamber for the corrosion tests was assembled, which delivered homogeneous vapor diffusion and drop deposition. Three bi-component bronzes, with 3%, 7% and 20% tin content, were subjected to seven days of controlled wet and dry cycles, and analyzed at precise intervals. Electrochemical impedance spectroscopy and spectrocolorimetry results were combined to show the different phases of corrosion. The patinas on all three samples at the end of the exposure period were studied with scanning electron microscopy to show the morphology of corrosion products; they were also analyzed by X-ray diffraction. The sample containing 7% tin produces a patina that is unstable and frequently dissolved. Partial patina dissolution also occurs during exposure for the 3% tin sample, but the effects are less pronounced. Because it reacts the least with the environment, the 20% tin sample demonstrates intermediate behavior (between the 7% and the 3% tin samples). However, the patina is less protective than the 3% tin sample patina.

1. INTRODUCTION

Bronze, an alloy composed mainly of copper and tin, has long been prized for the range of its possible alloy compositions. The properties of bronze depend on the concentration of the main components (copper and tin) and any additional alloying elements. The prehistoric and pre-classic

bronzes (Mesopotamian, Egyptian, Cretan, etc.) were low in tin content, and consisted of 90%-95% copper [1]. Ancient Roman bronze alloys contained about 70% copper, and lead and zinc were used in addition to tin. This composition of 70% copper and 30% white element was also common during the Middle Ages. The copper content increased during the Renaissance, when brass was developed by alloying zinc with copper [2-4].

Many European cities contain a wide variety of bronze artifacts, both of ancient and modern origin, which are often displayed outdoors. Accordingly, corrosion of these artifacts due to exposure to the urban environment, most significantly urban pollution, is of concern [5-6]. In particular, studies have examined the properties of pollutants (water solubility, chemical reactivity, acidity, deposition velocity) [6-7], air quality [4, 8-11], and the synergistic effects of pollutant mixtures [8-12]. The conservation state of specific artifacts exposed to polluted urban environments is commonly evaluated by their patina properties and the degradation of the bronze material [13-18]. Regardless of the focus of the research (pollutants, the bronze corrosion process, or the corrosion products), the relationship between the environment and material degradation products is unavoidable.

De la Fuente et al., for instance, combined environmental data (historical data and updates) with the "dose-response" of materials to produce a city scale assessment model for air pollution effects on the cultural artifacts (including bronzes) exposed to an outdoor environment [19]. Other research regarding the "dose-responses" involved monitoring the corrosion occurring in field tests [10, 20-24] or in laboratory tests (by immersion [25-26], dropping solutions [27], or exposure inside a spray-salt chamber cabinet [27-29]). Field tests require long exposure time and contain many factors/parameters that are difficult to quantify. In laboratory research, however, it is possible to precisely select, control and monitor the experimental parameters (including temperature, relative humidity, concentration of pollutants, the aggressiveness of the test), to focus on a specific phenomenon, and simulate and/or represent real cases.

This study differs from other studies in that laboratory testing was used to evaluate the effects of frequent wet and dry cycles of acid rain on bronze surfaces. The difference in corrosion behavior of the bronze alloys frequently used in artistic casting, and the acid rain corrosivity related to the wet and dry cycles and to the drop deposition, were examined systematically using a spray chamber to create an accelerated aging environment. This research also proposes the combination of electrochemical measurements (open circuit potential and impedance spectroscopy) and spectrocolorimetry to identify the different phases of corrosion. The latter technique, which is frequently used for the characterization of paintings and pigments, and less for the characterization of metal artefacts, was used not only to characterize the patina colour but also to describe the evolution of the corrosion.

2. EXPERIMENTAL

2.1. Material

Bronze alloys with low, medium and high tin content were selected. Their tin concentration is 3%, 7% and 20%, respectively; the concentration of copper and secondary alloy elements are shown in

Table 1 [30]. The alloys were cut into discs with a diameter of 12 mm and a thickness of 2 mm. Their surface was polished with abrasive papers of 400–1200 grade. They were then cleaned with 10 vol% sulfuric acid, rinsed with distilled water and degreased with acetone.

Table 1. Composition of the three copper alloys used (in mass %) [30].

Sample (tin concentration	Cu	Sn	Pb	As	Zn	Fe	Mn	Ni	S	Sb
3%	rest	3.0	0.2	0.2	0.2	0.2	0.2	0.2	0.2	0.2
7%	rest	7.0	0.2	0.2	0.1	0.3	0.3	0.5	0.5	0.7
20%	rest	22.5	0.2	0.2	0.2	0.2	0.2	0.2	0.2	0.2

2.2. Spray chamber test

A chamber for the corrosion tests was assembled in order to have a homogeneous vapor diffusion and deposition. The position of the vapor exit hole in the chamber (volume: 45 cm^3) and the flow rate of the vapor were optimized for drop deposition to avoid the formation of a water film on the surface of the sample. The discs were installed on columns 2 cm high, inclined at 45° and positioned 1.5 cm apart to avoid contamination between samples (Figure 1).

Figure 1. Photographs of the spray chamber for the corrosion tests.

Wet and dry cycles were performed six times per day, spraying 0.66 mL of vapor (synthetic solution of acid rain, the composition of which is reported in Table 2) per cycle. The daily wet and dry cycles were carried out as follows: 30 minutes between the first three vaporizations; 2 hours between the third and fourth vaporization; 30 minutes between the fourth, fifth and sixth vaporizations; 17 hours between the last vaporization of one day and the first vaporization of the following day. After seven days of cycles, the samples were dried for two days. In order to simulate an urban environment,

synthetic acid rain was sprayed on the samples. Figure 2 shows the graphs of the relative humidity (RH%) during the wet and dry tests performed at 25°C.

Table 2. Synthetic acid rain composition [28].

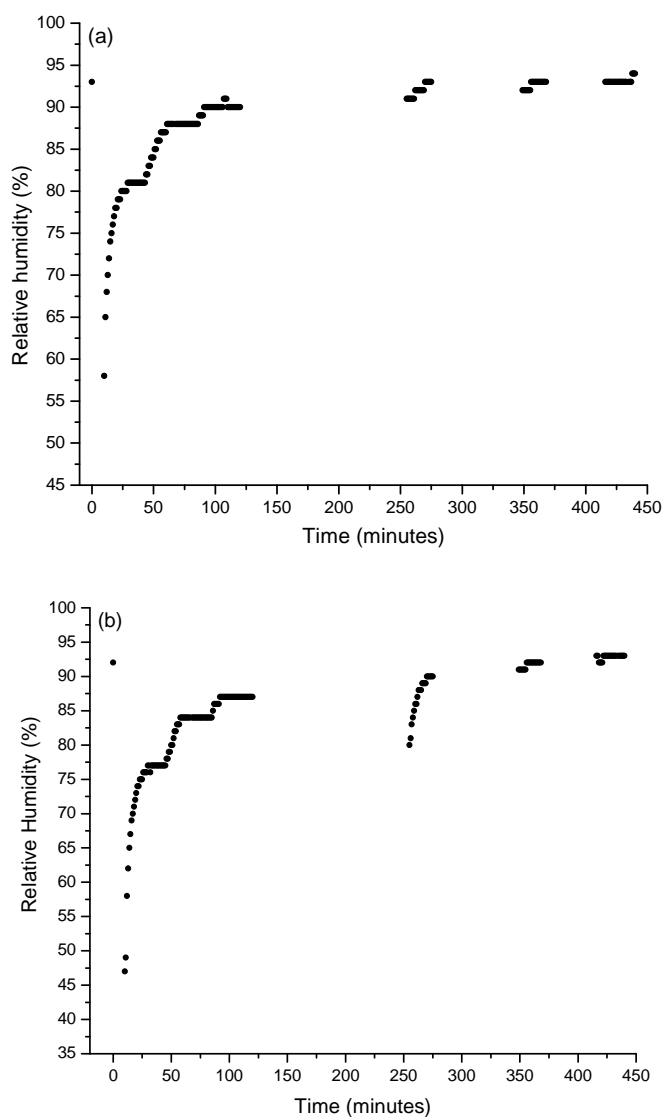| Component	(mg/dm^3)
H_2SO_4 (96%)	31.85
$(NH_4)_2SO_4$	46.20
$Na_2 SO_4$	31.95
HNO_3 (70%)	15.75
$NaNO_3$	21.25
NaCl	84.85

Figure 2. Relative humidity during the wet and dry tests in the vapor chamber: (a) during the week; (b) after the weekend.

2.1. Methods

Open circuit potential (OCP) monitoring, electrochemical impedance spectroscopy (EIS) and spectrocolorimetry measurements were done after 2 hours, 4 hours, 24 hours, 48 hours, 96 hours, 240 hours of wet and dry cycles to monitor the corrosion evolution. OCP and EIS measurements were done using an Autolab PGStat 20 instrument with a three electrode cell: Ag/Ag/Cl (reference electrode), Pt (counter electrode) and bronze (working electrode) in a solution of 0.1 M of sodium sulfate. The impedance setup was performed from 75 kHz to 1 Hz at 10 mV.

The EIS parameters were correlated to the patina properties as following:

− the patina passivity was determined from the film resistance (R_f). Sometimes, the film resistance can be distinguished by the charge transfer or total system resistance. However, the total resistance (R_t) of the system relates to the decreased rate of the corrosion progress [31-32];

− the corrosion process progress was deduced from resistance and capacity of charge transfer (R_{ct}; C_{ct}). The higher the value of R_{ct} and the lower the value of C_{ct}, the slower the corrosion and the more passive is the surface analyzed [31-32];

− the diffusion phenomena as well as the patina porosity are shown by the Warburg element (W) [31-32];

− the CPE (constant phase element) shows the inhomogeneous character of the system, frequently considered as electrode roughness and related to the capacitance (Q) [31-32].

The results are represented by the Nyquist diagrams that show the mass-transport contribution in the lower frequency range, the charge transfer process at middle frequency arcs, and the corrosion products formed in the high frequency range [33].

Colorimetric measurements were carried out with a portable spectrophotometer X-Rite SP64. The reflected light percentage (%) was measured as a function of the wavelength (nm). The reflectance curves and the lightness (L^*) are used to explain the patina formation and its growth. These parameters can distinguish small differences and can therefore highlight small patina evolution.

The color difference (ΔE) between two measurements was calculated based on the difference between colorimetric parameters L* (lightness), a* (red-green component) and b* (yellow-blue component) using the following equation [34]:

$$\Delta E = \sqrt{\left(\Delta L^*\right)^2 + \left(\Delta a^*\right)^2 + \left(\Delta b^*\right)^2}$$

The color difference (ΔE) is used to describe the corrosion rate: relevant ΔE values indicate a large color change associated with fast corrosion that produces a patina with a color that differs from the surface color previously analyzed. ΔE is also an index of color damage (color difference from the natural alloy's color). The variation of ΔE over time can be used to estimate the patina's evolution and stability. The color difference can be correlated both to the patina formation and to the patina dissolution. The dissolution process occurring on the film is an indicator of an unstable or poorly passivating patina.

Scanning electron microscopy (SEM) images were taken to study the morphology of the corrosion products and their growth. The instrument used in this research is a HITACHI S 2500,

equipped with a LaB_6 electron source and a scintillation electron photo detector. The typical working pressure was 10^{-7} mbar.

In addition X-ray diffractograms were used to characterize the corrosion products. A Thermo Scientific* ARL X'TRA powder diffractometer was used with the following setup: 40 kV, 40 mA, scanning 2θ from $10°$ to $80°$ grade, step width of $0.02°$ and counting time of 5 seconds per step.

3. RESULTS AND DISCUSSION

3.1. OCP monitoring

The OCP monitoring of the three alloys exposed to acid rain spray is shown in Figure 3. The sample with 3% tin shows a potential decrease between the 2nd and 4th hour of exposure in the chamber. The potential variation can be related to the absence and presence of SnO_2, as was also observed by De Oliveira et al. [20]. Afterward the 4th hour, the potential increases towards anodic values due to the formation of corrosion products [35]. The patina undergoes a slight dissolution between the 24th to 48th hour. Afterward the 96th hour, the potential is stable, which indicates a stable patina.

In the 7% tin sample, the potential increases steadily until the 240th hour. The anodic process of patina formation continues until the 240th hour, with the only interruption at around 96th hour. The patina barrier properties improve throughout the exposure tie. According to Cicileo et al. [35], the most protective products, which are adherent and non-porous at the surface, give a stable potential or a slight potential increase with time; on the other hand, a potential decrease indicates less protective products on the surface.

The 20% tin samples show a high corrosion process (patina formation) of the alloy until the 48th hour, followed by a short time of stability and then by cathodic dissolution of the patina.
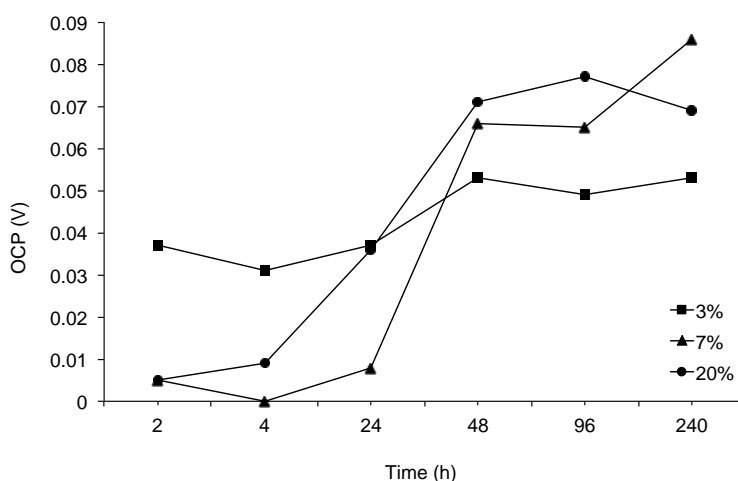

Figure 3. OCP measurements of 3%, 7% and 20% tin bronzes sprayed with a synthetic solution of acid rain for 2 hours, 4 hours, 24 hours, 48 hours, 96 hours, 240 hours.

3.2. EIS measurements

Figure 4 shows the Nyquist graphs of the three alloys exposed to acid rain vapor from 0 up to 240 hours. It was sometimes difficult to distinguish the various electrochemical elements (for example to distinguish the patina's resistance from the charge transfer resistance or to distinguish the film capacity from the C of the charge transfer). It was also difficult to give a linear interpretation of the patina formation over time due to the inhomogeneity of the patina formed.

On the 3% tin sample, the corrosion rate increases until the 4th hour. The semi-circle opening up during the 24th hour shows the passive property of the layer, probably due to the presence of SnO_2 and Cu_2O in accordance with the copper Pourbaix diagram and others studies [20, 33, 36-38]. The layer, however, is damaged due to the aggressiveness of the acid rain vapor during the 48th hour, and accordingly the OCP decreases. In the last hours (96-240 hour) the passive patina properties improve, reaching highest resistance values at 240th hour, as the indicated by the radius of the semi-circle.

The 7% tin sample shows a gradual decrease in corrosion during the first 4 hours. Between the 24th and 48th hours, the patina barrier properties improve, as already demonstrated with OCP measurements. During the 96th hour, the Nyquist curve closes, which indicates that some corrosion processes resume on the metal surface. These processes produce a layer of corrosion products and continue during the 240th hour.

On the 20% tin sample, the corrosion reaction produces a layer that progressively slows down the corrosion up until the 48th hour. A new corrosion process restarts on the surface, adding to the existing patina.

The equivalent circuits that are better fit to explain this interpretation are reported in Table 3.

On the 3% tin sample, the corrosion process is expressed by the circuit $R_e(R_tQ)W$ during the 2nd exposure hour. The circuit of the 4th hour is more complex: $R_e(R_fQ)(R_{ct}C)W$. In this last circuit, the film with higher resistance value ($9.85*10^5$ Ω instead of the previous 363.64 Ω) along with the lower capacity ($2.89*10^{-9}$ F instead of the previous $5*10^{-4}$ F) allows for both charge transfer and mass diffusion on the double layer as already demonstrated by Sandberg et al. and Payer et al. [32, 39]. These processes have a slight increase during the 24th hour and lead to a $R_e(R_tQ)W$ circuit where fewer terms (equivalent circuit elements) are detected but the diffusion process is still revealed. In the last hours (96th to 240th hour), the resistance increase ($R_{240h}=7.49*10^8$ Ω) suggests that a more homogeneous and stable patina is formed.

On the 7% tin sample, the resistance increases while the Warburg diffusion decreases (and goes to zero during the 24th hour). The corrosion process is therefore dominated by charge transfer (Q). A resistance values increase is detected between 24th and 48th hours of the chamber exposure, and is consistent with the increase of the potential revealed by the OCP measurements. The total resistance reaches $1.92*10^8$ Ω. Afterward the 48th hour, a partial dissolution of the layer reduces the resistance and exposes the surface to corrosion up until the 240th hour.

The 20% tin sample shows an equivalent circuit composed of two distinct parts. The film and the charge transfer coexist during exposure. At the 96th hour, the Warburg element also appears. The film resistance increases until the 4th hour, and then decreases until the 240th hour ($R_{2h}=5.60$ Ω; $R_{4h}=1*10^6$ Ω; $R_{48h}=8.71*10^3$ Ω; $R_{96h}=7.24*10^3$ Ω; $R_{240h}=8.08*10^2$ Ω).
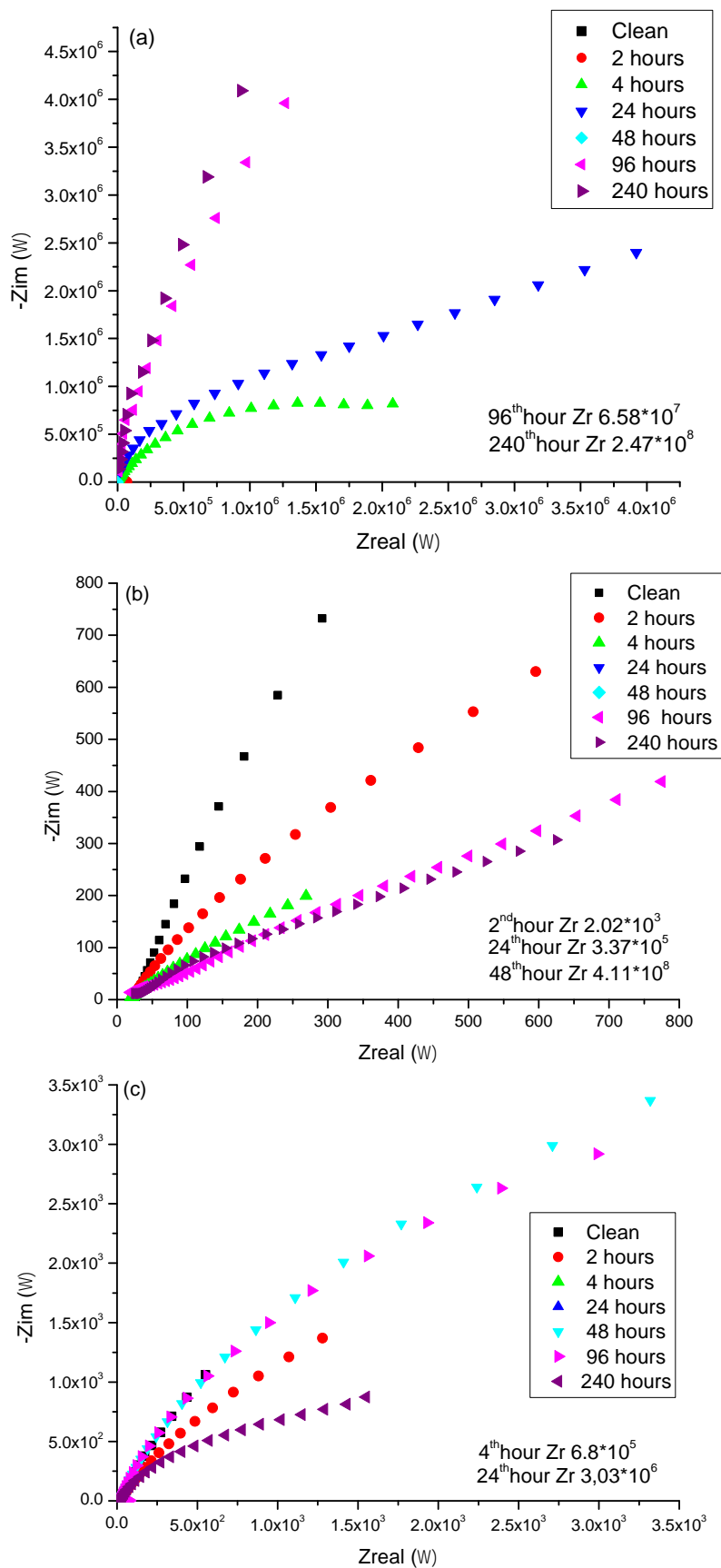
Figure 4. EIS results—samples in a chamber sprayed with a synthetic solution of acid rain for 2 hours, 4 hours, 24 hours, 48 hours, 96 hours, 240 hours. (a) 3%, (b) 7% and (c) 20% tin samples.

Table 3. Overview of the equivalent equivalent circuits that have been used to fit the data.

3% Sn					
Clean	R=26.22			Q=$3.65*10^{-4}$	
	R_eQ				
2 hours	R=22.61	R=363.64		Q=$5*10^{-4}$	W=925.3
	$Re(R_tQ)W$				
4 hours	R=844.42	R=$9.86*10^5$	Q=$2.09*10^{-9}$	R=$9.32*10^5$	C=$8.75*10^{-9}$	W=$1.12*10^6$
	$R_e(R_fQ)(R_{ct}C)W$				
24 hours	R=839.4	R=$7.75*10^5$	Q=$2.1*10^{-8}$	R=$2.94*10^{-13}$	Q=$4.16*10^{-7}$	W=$7.96*10^6$
	$R_e(R_fQ)(R_{ct}Q)W$				
48 hours	R=22.61	R=363.64		Q=$5*10^{-4}$	W=925
	$R_e(R_tQ)W$				
96 hours	R=$7.8*10^4$	R=$5.33*10^7$		Q=$2*10^{-10}$	
	$Re(R_tQ)$				
240 hours	R=$5.21*10^5$	R=$7.49*10^4$		Q=$3.65*10^{-10}$	
	$Re(R_tQ)$				

7% Sn					
Clean	R=24.5			Q=$2.28*10^{-4}$	
	R_eQ				
2 hours	R=18.76	R=31.33	Q=$3.87*10^{-4}$	R=$1.99*10^3$	C=$3.60*10^{-4}$	W=$6.48*10^3$
	$R_e(R_fQ)(R_{ct}C)W$				
4 hours	R=18.57	R=191.59	Q=$5.04*10^{-4}$	R=120.9	C=$2.83*10^{-5}$	W=702.4
	$R_e(R_fQ)(R_{ct}C)W$				
24 hours	R=146.5	R=$1*10^6$	C=$2.83*10^{-8}$	R=$3.64*10^5$	Q=$4.25*10^{-8}$	
	$R_e(R_fC)(R_{ct}Q)$				
48 hours	R=$1.08*10^6$	R=$1.92*10^8$		Q=$4.33*10^{-11}$	
	$R_e(R_tQ)$				
96 hours	R=2.85	R=$5.73*10^3$	Q=$5*10^{-4}$	R=13.59	C=$6.42*10^{-7}$	
	$R_e(R_fQ)(R_{ct}C)$				
240 hours	R=17.09	R=$1.77*10^3$		Q=$4.4*10^{-4}$	
	$Re(R_tQ)$				

20% Sn					
Clean	R=2.93		R=$15.78*10^3$		Q=$2*10^{-4}$	
	$R_e(R_tQ)$				
2 hours	R=13.31	R=5.60	Q=$1.58*10^{-4}$	R=$1.24*10^3$	C=$9.92*10^{-6}$	W=$1.16*10^3$
	$R_e(R_fQ)(R_{ct}C)W$				
4 hours	R=623.4	R=$1*10^6$	C=$7.31*10^{-9}$	R=$3.01*10^5$	Q=$1.58*10^{-8}$	
	$R_e(R_fC_f)(R_{ct}Q_{ct})$				
24 hours	R=$6.24*10^6$			Q=$1.21*10^{-9}$	
	ReQ				
48 hours	R=$2.18*10^{-13}$	R=$8.71*10^3$	Q=$3.19*10^{-5}$	R=20.4	C=$1.34*10^{-8}$	
	$R_e(R_fQ)(R_{ct}C)$				
96 hours	R=15.07	R=$7.24*10^3$	C=$2.06*10^{-5}$	R=996	C=$1.96*10^{-5}$	W=$1*10^3$
	$R_e(R_fC)(R_{ct}C)W$				
240 hours	R=20.15	R=808	C=$7.82*10^{-5}$	R=518	C=$9.78*10^{-5}$	W=$3.55*10^3$
	$R_e(R_fC)(R_{ct}C)W$				

The patina is formed during the exposure, but its passivation properties do not improve over time; charge transfer is always present.

In conclusion, on the 3% tin sample the passive patina properties improve progressively, reaching the highest resistance values at the 240th hour. This alloy is more protected and undergoes less corrosion by the solution than the 7% and 20% tin samples according to the OCP results and to the above-mentioned description by Cicileo et al. [35].

3.3. Spectrocolorimetry

The color evolution of the three alloys was examined over the course of 10 days. Figure 5 shows the reflectance curves as a function of time. The reflectance curves show a relatively large difference between the clean sample and two hours of chamber exposure for the 3% and 7% tin samples, while only a small variation for the 20% tin sample was detected. The reflectance decrease can be correlated to the corrosion rate that occurs more quickly for the first two alloys, and more slowly for the 20% tin sample. In the 3% and 7% tin samples, the corrosion is most rapid in the first hours. It is worth noting that the reflectance loss for the 3% and 20% tin sample is greater after 2 hours of exposure than after 4. This is probably due to an inhomogeneity of the patina and to its instability in the first phase of formation.
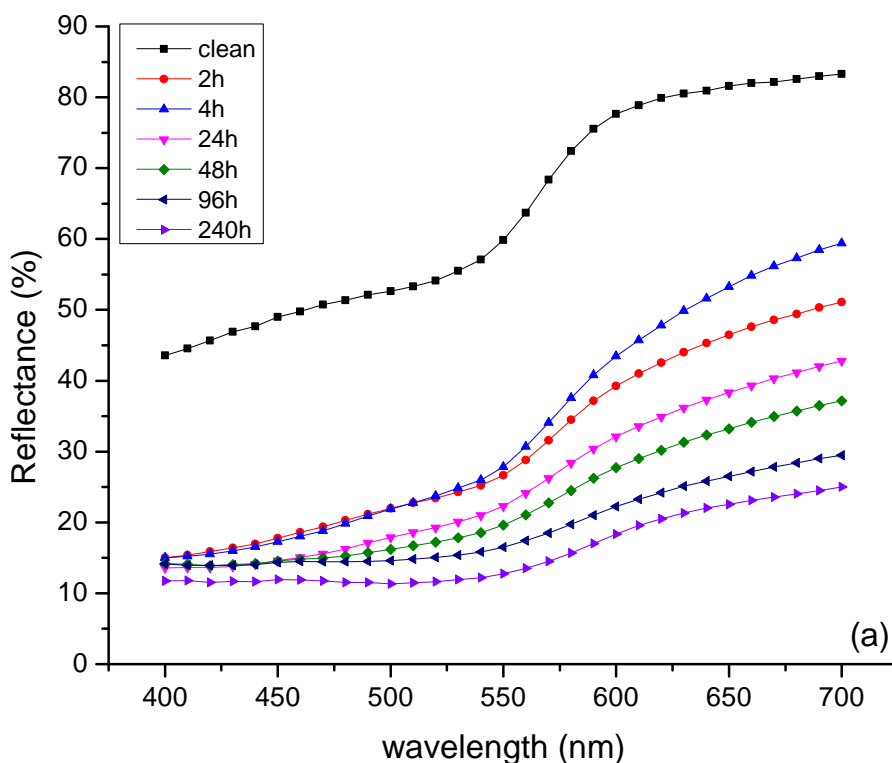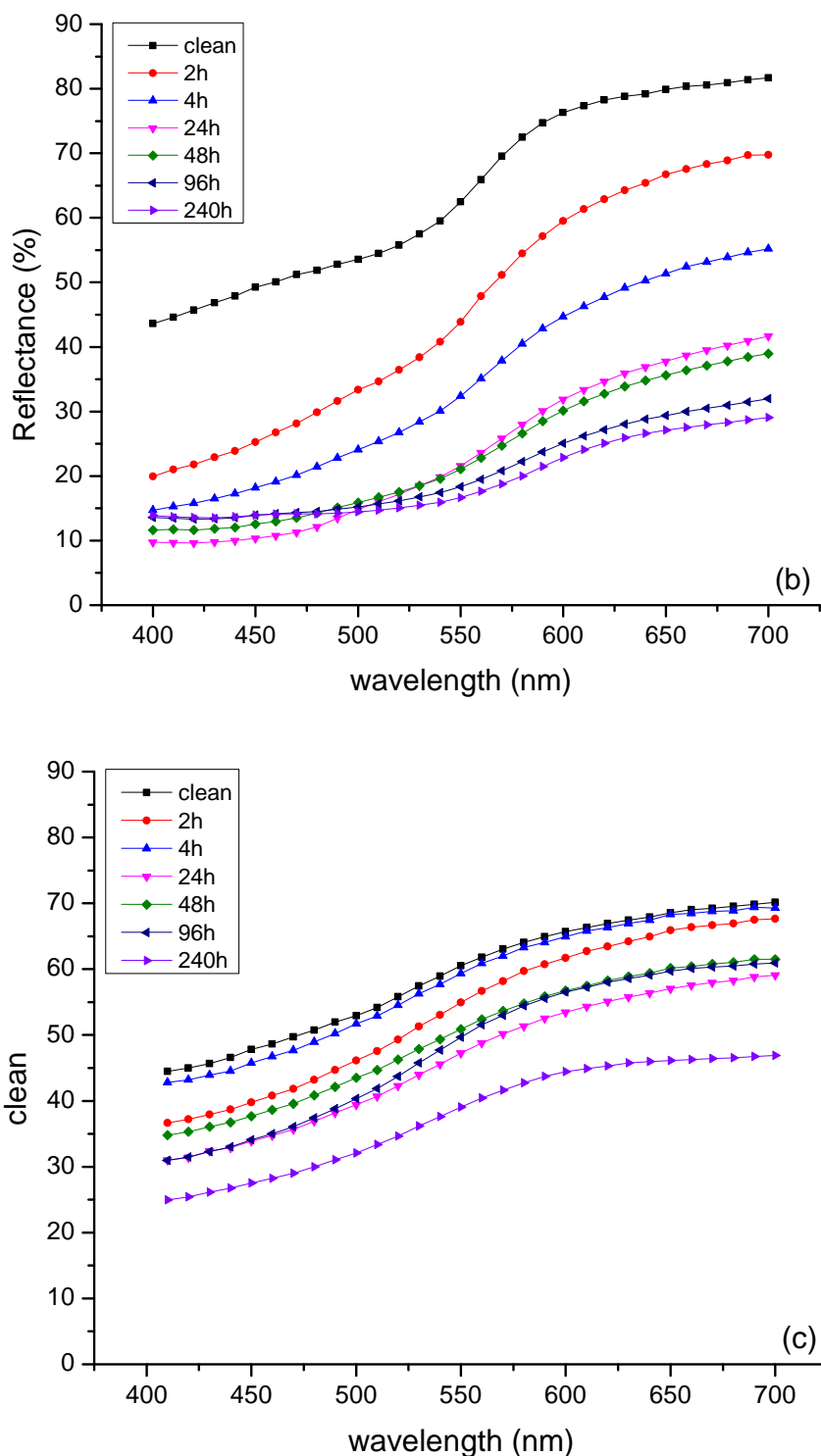
Figure 5. Reflectance measurements in chamber on samples sprayed with a synthetic solution of acid rain for 2 hours, 4 hours, 24 hours, 48 hours, 96 hours, 240 hours. (a) 3%, (b) 7% and (c) 20%.

The lightness values of the three samples have an inverse trend with respect the OCP variation: when the OCP values decrease the L* value increases, while when an anodic process produces a film

the lightness decreases. The a^*, b^* and C^* parameters describe the color of the patina formed during the test steps (see Table 4).

Table 4. CIEL* a* b* parameters in chamber on samples sprayed with a synthetic solution of acid rain for 2 hours, 4 hours, 24 hours, 48 hours, 96 hours, 240 hours.

3% Sn				
Time	L^*	a^*	b^*	C^*
0h	83.63	10.35	14.17	17.55
2h	61.06	12.38	19.73	23.30
4h	62.66	15.25	23.44	27.96
24h	56.26	11.54	18.61	21.89
48h	53.26	11.07	13.98	17.83
96h	49.31	9.39	8.05	12.37
240h	44.57	10.98	6.53	12.78

7% Sn				
Time	L^*	a^*	b^*	C^*
0h	84.07	8.26	14.63	16.80
2h	73.31	11.30	26.52	28.83
4h	64.85	11.21	25.18	27.56
24h	54.92	12.60	27.04	29.83
48h	54.48	11.43	20.56	23.53
96h	51.38	9.79	12.40	15.80
240h	49.55	9.88	9.33	13.59

20% Sn				
Time	L^*	a^*	b^*	C^*
0h	81.76	2.99	11.94	12.31
2h	78.71	4.35	15.65	16.25
4h	81.17	3.21	13.00	13.39
24h	74.09	4.42	15.38	16.01
48h	76.36	3.74	14.23	14.71
96h	75.45	4.64	17.40	18.01
240h	68.48	4.10	15.09	15.63

Comparing the evolution of the ΔE values (Figure 6), the 3% and 7% tin samples show a non-linear corrosion process. In this work the ΔE values were correlated to the corrosion rate and to the patina properties. The 3% sample has a stable patina in the first 24 hours, the 7% tin sample is more damaged during this period. After the 24th hour, the situation is reversed, even if the color difference between the two alloys is less marked. The 20% tin sample is the least changed, as the ΔE between the color of the natural alloy and the color at the end of the test indicates.
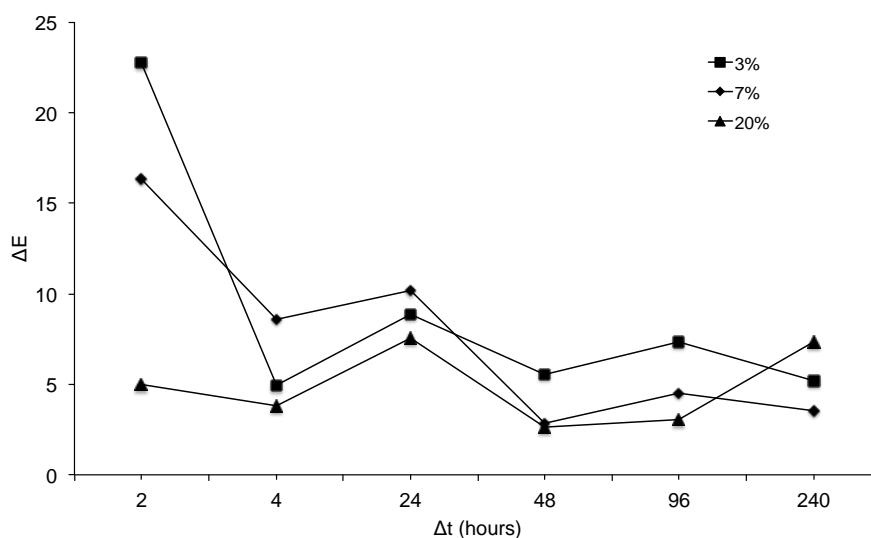
Figure 6. Color differences during the exposure of the three alloys to acid rain vapor.

3.4. SEM and X-ray diffraction

Figure 7 shows the SEM images taken for the 3%, 7% and 20% tin samples after 240 hours of chamber exposure to acid rain vapor. Overall, the surface of the 20% tin sample is the least covered by corrosion products. Also, the morphologies of the corrosion products are different: on the 3% tin sample, the patina is largely formed and on the 7% tin sample, it contains some almost perfectly cubic crystals. The slight patina formed on the 20% tin sample is more "granular."
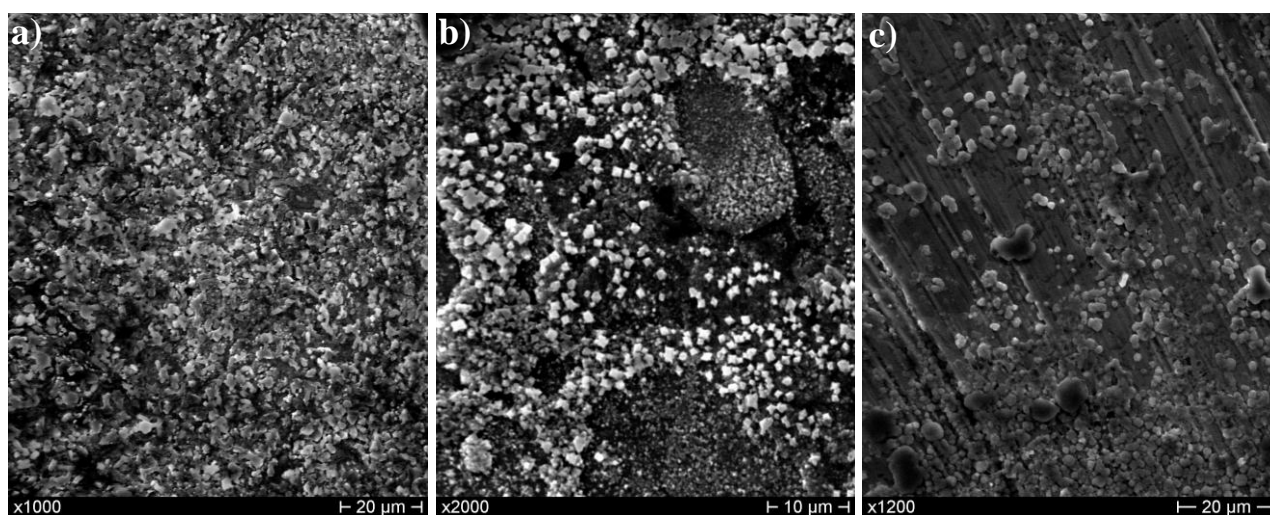

Figure 7. SEM secondary electrons images of a) 3%, b) 7% and c) 20% tin samples after 240 hours of exposure to acid rain vapor.

In order to support the qualitative analysis and to identify the composition of the corrosion products, X-ray diffraction (XRD) analysis was performed on the samples after the 240th hour of

exposure. Figure 8 shows the XRD spectra and demonstrates the presence of cuprite (Cu_2O) and cassiterite (SnO_2) presence on the 3% and 7% tin samples. In neither the 3% nor the 7% diffractograms did sulfur compounds appear in the XRD. However, sulfur was detected with EDS in both 3% and 7% tin samples, indicating that the sulfur content was below the limit of XRD detection. These data indicate that some sulfur compound is in its first phase of formation on 3% and 7% tin samples. On the 20% tin sample, cuprite (Cu_2O) is present along with some gherardite crystal ($Cu_2(NO_3)(OH)_3$.
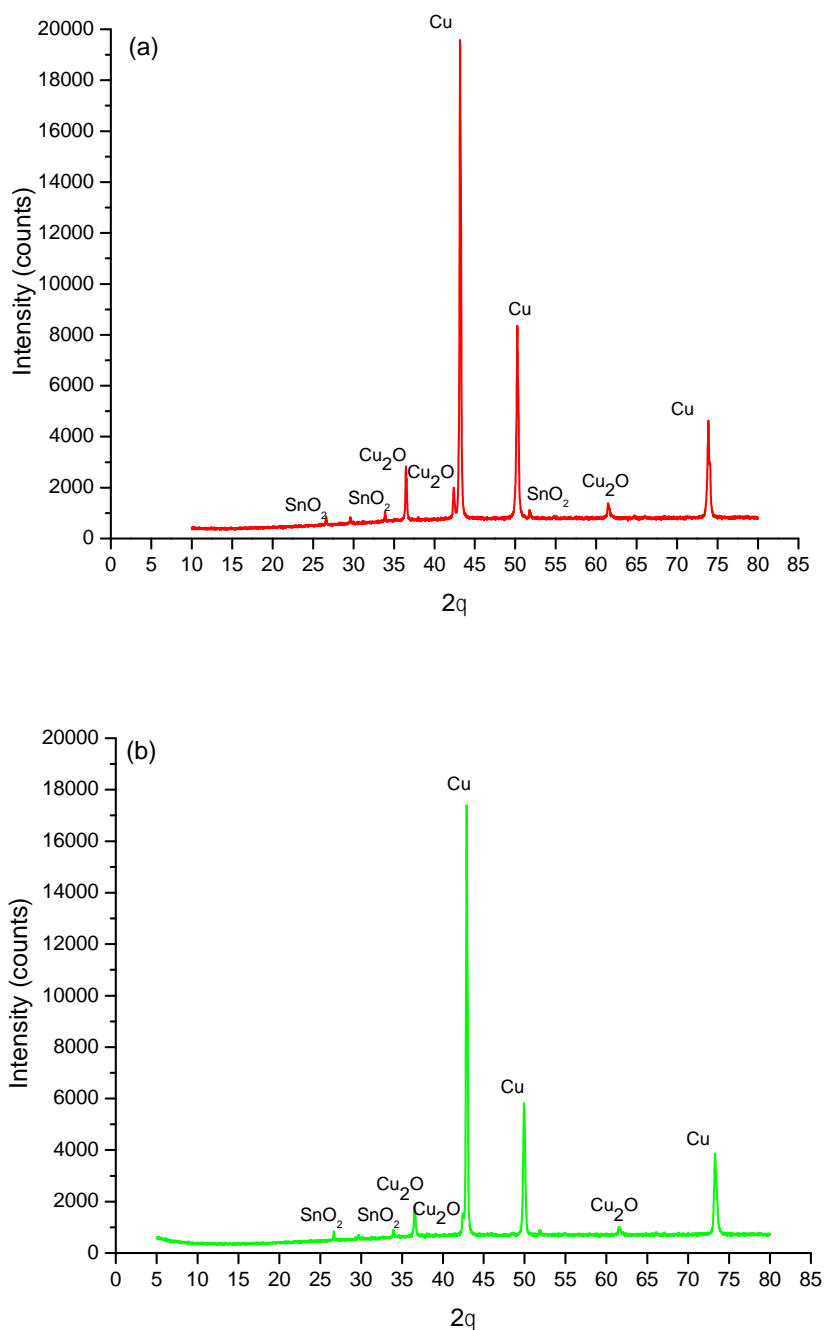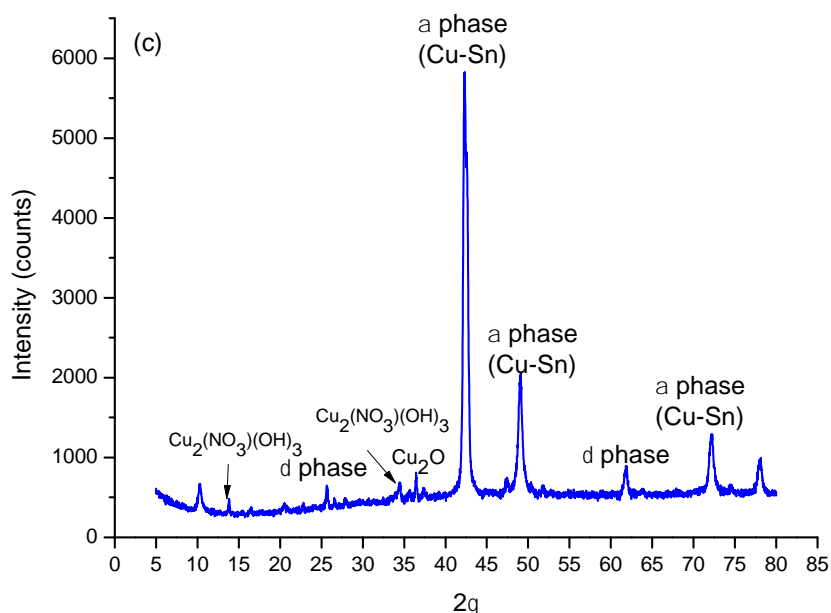
Figure 8. XRD data of the three samples (a) 3%, (b) 7% and (c) 20% after 240 hours of exposure.

4. CONCLUSIONS

With OCP measurements we found that the more unstable patina grows on the 7% and 20% tin samples. These results were confirmed by EIS: on the 7% tin sample, the patina is unstable and frequently dissolved. Also, the 3% tin sample patina is partially dissolved during the exposure but the effects are less pronounced. For the 20% tin sample, the SEM images and color analysis shows the surface to be less damaged but the patina formed is also less protective than the 3% tin sample patina.

Spectrocolorimetry measurements and SEM imaging supported the electrochemical data interpretations: the 3% tin sample shows more color changes due to more developed patina (compared to the 7% and 20% tin sample patinas). The color difference variation is due to the patina nature, growth and/or dissolution but also to the inhomogeneity of the layers. For this reason the color analysis of the 3% tin sample appears in the negative range of corrosion behavior. The results of the OCP, EIS and spectrocolorimetry are consolidated in Figure 9, where the electrochemical properties (passivity and/or stability) are compared to the color differences. A more passive and stable (or thicker) patina protects the alloy from the corrosion progress, so the sample will be located nearest the positive side of the arrow in that graph. This schematic graphic is intended to serve as a tool that could allow to different professionals in cultural heritage conservation to better understand and make use of the findings of this research.
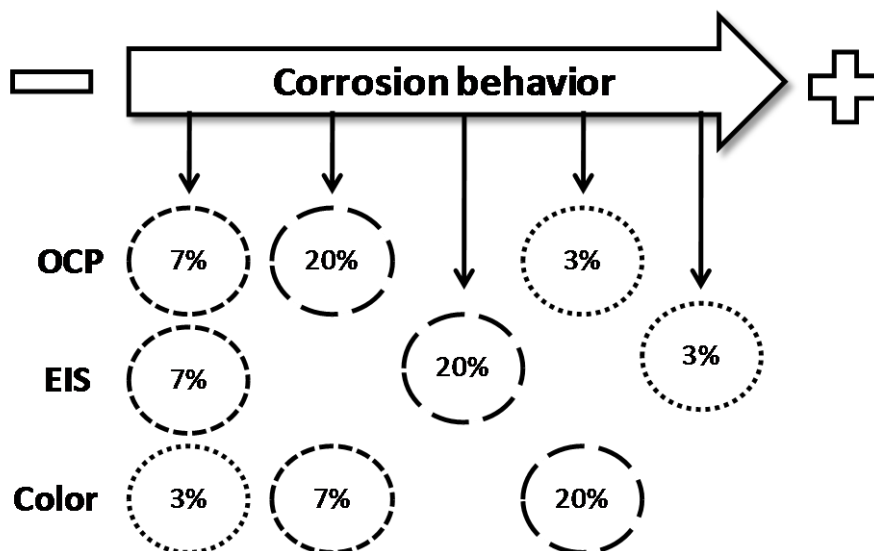
Figure 9. The "damage scale" for the three alloys sprayed with acid rain for 240 hours.

References

1. I. De Ryck, A. Adriaens and F. Adams, *J. Cult. Heritage* 61 (2005) 261.
2. G. Giubbini, in *Le Tecniche Artistiche* (Ed. E. Baccheschi, C. Dufour Bozzo, F. Franchini Guelfi, G. Gallo Colonni, E. Gavazza, G. Giubbini, M. Leva Pistoi, E. Parma Armani, F.R. Pesenti, F. Sborgi), Mursia, Milano (1991) pp. 33.
3. F. Habashi (Ed.), *A History of Metallurgy*, Métallurgie Extractive Québec, Québec City, Canada (1994)
4. D.A. Scott, J. Podany and B. B. Considine (Eds.), *Ancient and Historical Metals: Conservation and Scientific Research*, Getty Institute Publication, Los Angeles (1994).
5. J. Watt, J. Tidblad, V. Kucera and R. Hamilton (Eds.), *The Effects of Air Pollution on Cultural Heritage*, Springer, New York, Heidelberg (2009).
6. C. Leygraf and T.E. Graedel, *Atmospheric Corrosion*, The Electrochemical Society, Inc., Pennington, New Jersey (2000).
7. C. Leygraf, in *Corrosion Mechanisms in Theory and Practice* (Ed. P. Marcus), 2nd Edition, CRC Press, France (2002) pp. 529.
8. S. Oeschen and M. Faller, *Corros. Sci.* 39(9) (1997) 1505.
9. H. Strandberg and L.G. Johansson, *J. Electrochem. Soc.*, 144(7) (1997) 2334.
10. F. Samie, J. Tidblad, V. Kurcera and C. Leygraf, *J. Electrochem. Soc.* 154(5) (2007) C249.
11. J. Tidblad and C. Leygraf, *J. Electrochem. Soc.*142(3) (1995) 749.
12. J.E. Svensson and L.G. Johansson, *J. Electrochem. Soc.* 140(8) (1993) 2210.
13. C. Chiavari, K. Rahmouni, H. Takenouti, S. Joiret, P. Vermauta and L. Robbiola, *Electrochem. Acta* 52 (2007) 7760.
14. G. D'Ercoli, G. Guida, M. Marabelli and V. Santin, in *Cultural Heritage Conservation and Environment Impact Assessment by Non-Destructive Testing and Micro-Analysis* (Eds. R. Van Grieken and K. Janssens), Taylor & Francis Group, London (2005) pp. 19.

15. R. Petriaggi (Ed.), *Il Satiro danzante*, Leonardo International, Milano (2003).
16. P. Letardi, I. Trentin and G. Cutugno, *Monumenti in Bronzo all'Aperto. Esperienze di Conservazione a Confronto*, Nardini Editore, Firenze (2004).
17. P. Dilmann, G. Béranger, P. Piccardo and H. Matthiesen, *Corrosion of Metallic Heritage Artifacts. Investigations, Conservations, and Prediction for Long-Term Behaviour*, Woodhead Publishing Materials, Cambridge (2007).
18. M. Ryhl-Svendsen, *J. Cult. Heritage* 9 (2008) 285.
19. D. de la Fuente, J.M. Vega, F. Viejo, I. Dìaz and M. Morcillo, *Atmos. Environm.* 45 (2011) 1242.
20. F.J.R. De Oliveira, D.C.B. Lago, L.F. Senna, L.R.M. De Miranda and E. D'Elia, *Mat. Chem. Phys.* 115 (2009) 761.
21. M. Watanabe, Y. Higashi and T. Ichino, *J. Electrochem. Surf.* 150(2) (2003) B37.
22. A.G. Nord, K. Tronner and A.J. Boyce, *Water Air Soil Poll.* 127(1-4) (2001) 193.
23. G. Laguzzi, L. Luvidi and G. Brunoro, *Corros. Sci.* 43 (2001) 747.
24. J. Sandberg, I.O. Wallinder, C. Leygraf and N. Le Bozec, *Corros. Sci.* 48 (2006) 4316.
25. E. Sidot, N. Souissi, L. Bousselmi, E. Triki and L. Robbiola, *Corros. Sci.* 48 (2006) 2241.
26. L. Morselli, E. Bernardi, C. Chivari and G. Brunoro, *Appl. Phys. A* 79 (2004) 363.
27. C. Chiavari, E. Bernardi, F. Ospitali, L. Robbiola, C. Martini and L. Morselli, La Metallurgia Italiana (2009) Maggio 2009.
28. C. Chiavari, A. Colledan, A. Frignani and G. Brunoro, *Mat. Chem. Phys.* 95 (2006) 252.
29. T. Kosec, H. Otmacić Ćurković and A. Legat, *Electrochim. Acta* 56 (2010) 722.
30. C. Ingelbrecht, A. Adriaens and E.A. Maier, *Certification of arsenic, lead, tin and zinc (mass fractions) in five copper alloys CRM 691*, EUR 19778/1, Office for Official Publications of the European Communities, Luxembourg (2001)
31. W.A. Badawy, R.M. El-Sherif and H. Shehata, *J. Appl. Electrochem.* 37 (2007) 1099.
32. J. Sandberg, I.O. Wallinder, C. Leygraf and N. Le Bozec, *Corros. Sci.* 48 (2006) 4316.
33. N. Souissi, L. Bousselmi, S. Khosrof and E. Triki, *Mater. Corros.* 54 (2003) 318.
34. E. Franceschi, P. Letardi and G. Luciano, *J. Cult. Heritage* 7 (2006) 166.
35. G.P.Cicileo, M. A.Crespo, B. M. Rosales, *Corrosion Science* 46 (2004) 929-953.
36. A. Krätschmer, I. Odnevall Wallinder, Cristofer Leygraf, *Corrosion Science*, 44 (2002), 425-450;
37. B. M. Rosales, R. M. Vera, J. P. Hidalgo, *Corrosion Science* 52 (2010) 3212-3224;
38. Y. Surme, A.A. Gurten, E. Bayol, E. Ersoy, *Journal of alloys and compounds* 485 (2009) 98-103;
39. J.H. Payer, G. Ball, B.I. Rickett, H.S. Kim, *Material Science and Engineering* A198 (1995) 91-10.